TOXICOLOGICAL SCIENCES **113(1)**, 127–137 (2010)
doi:10.1093/toxsci/kfp259
Advance Access publication November 3, 2009

Cadmium Induces Intracellular Ca^{2+}- and H_2O_2-Dependent Apoptosis through JNK- and p53-Mediated Pathways in Skin Epidermal Cell line

Young-Ok Son,* Jeong-Chae Lee,†,‡ J. Andrew Hitron,* Jingju Pan,* Zhuo Zhang,* and Xianglin Shi*,[1]

*Graduate Center for Toxicology, College of Medicine, University of Kentucky, Lexington, Kentucky 40536-0305; †School of Dentistry and 21 Century Education Center for Advanced Public Dental Health (BK 21 program), Chonbuk National University, Jeonju 561-756, South Korea; and ‡Research Center of Bioactive Materials, Chonbuk National University, Jeonju 561-756, South Korea

[1] To whom correspondence should be addressed. Fax: (859) 323-1059. E-mail: xshi5@email.uky.edu.

Received August 10, 2009; accepted October 18, 2009

Cadmium is a toxic heavy metal and has been widely used in industry. The skin is an important target for this metal. The mechanisms by which cadmium leads to damage to the skin are unclear at present. The aims of this study were to examine whether cadmium induces apoptosis in mouse skin epidermal cell line, JB6 Cl41 cells, and to investigate the cellular mechanisms by which cadmium causes cytotoxicity in the cells. The present study showed that cadmium induced cell death by apoptosis in a dose-dependent manner, as proven by the appearance of cell shrinkage, the increase of Annexin V positively stained cells, and the formation of nuclear DNA ladders. Cadmium-induced apoptosis involved a mitochondria-mediated mechanism but not caspase-dependent pathway in that the critical apoptotic events induced by cadmium, such as the decrease of Bcl-2/Bcl-xL, the increase of GADD45α, and the nuclear translocation of apoptosis inducing factor, were not affected by the inhibition of executive caspases. In contrast, blockage of p53 and JNK by pharmacological inhibitors or small interference RNA transfection suppressed the cadmium-induced apoptosis with the concomitant inhibition of antiapoptotic Bcl-2 family proteins and GADD45α, respectively. Furthermore, the activation of p53 and JNK and their downstream proteins in cadmium-exposed cells were inhibited by individual treatment with catalase and Bapta-acetoxymethyl. These results suggest that cadmium induces apoptosis *via* the activation of JNK- and p53-mediated signaling, where calcium ion and hydrogen peroxide act as the pivotal mediators of the apoptotic signaling.

Key Words: **cadmium; skin epidermal cell; cytotoxicity; apoptosis; p53; JNK.**

Cadmium is a toxic heavy metal that is widely distributed in the earth's crust, air, and water. Major sources of cadmium exposure are food, cigarette smoke, and cadmium-related industries (Jarup, 2003). Cadmium has a very long biological half-life, which causes a cumulative toxic effect. Although cadmium accumulates primarily in the lung, liver, and kidney (Gerhardsson *et al*., 2002; Jarup, 2003), the skin is also easily exposed to the toxic metal.

It has been documented that cadmium-induced toxicity and carcinogenesis are closely associated with the production of reactive oxygen species (ROS) (Bagchi *et al*., 2000; Szuster-Ciesielska *et al*., 2000). Cadmium elevates the generation of ROS by depleting cellular glutathione and antioxidant enzymes, such as superoxide dismutase (SOD) and catalase (CAT) (Bagchi *et al*., 2000; Shaikh *et al*., 1999), even though it is considered a redox-inactive metal that does not catalyze a Fenton-type reaction (Ercal *et al*., 2001; Stohs and Bagchi, 1995). It has also been reported that cadmium produces ROS by inhibiting the electron transfer chain in the mitochondria (Wang *et al*., 2004).

Calcium ions play central roles in a variety of biological functions. It is likely that cadmium-mediated cytotoxicity is in part related to the intracellular calcium levels (Lemarie *et al*., 2004; Wang *et al*., 2008). This alteration of intracellular levels of calcium ion can cause apoptosis (Berridge *et al*., 1998). Indeed, high levels of intracellular calcium ion lead to the disruption of mitochondrial calcium equilibrium, which facilitates the loss of mitochondria membrane potential and eventually induces the formation of ROS (Lemarie *et al*., 2004; Wang *et al*., 2008). These observations suggest that calcium ion has important roles in cadmium-induced toxicity through the generation of ROS, although the cellular mechanism(s) by which cadmium involves calcium ions in its toxic action is unclear.

It is commonly accepted that cadmium induces cell death by apoptosis in cellular systems (Fujimaki *et al*., 2000; Watjen *et al*., 2002). However, cadmium induces apoptosis by either caspase-dependent (Hossain *et al*., 2009; Wang *et al*., 2009) or caspase-independent mechanisms (Mao *et al*., 2007; Shih *et al*., 2003) depending on the types of cells. Although cadmium-induced cytotoxicity and apoptosis are well studied in various cell types, the precise mechanisms are not well understood. In addition, the role of cadmium-induced apoptosis in skin epidermal cells has not been studied yet. We investigated the apoptotic signaling pathways for ROS and calcium ions generated by cadmium using mouse skin epidermal cell line, JB6 cells.

MATERIALS AND METHODS

Chemicals and laboratory wares. Unless specified otherwise, all chemicals and laboratory wares were purchased from Sigma Chemical Co. (St Louis, MO) and Falcon Labware (Bectone-Dickinson, Franklin Lakes, NJ), respectively. Eagle's minimal essential medium (EMEM), fetal bovine serum (FBS), gentamicin, and L-glutamine were purchased from Gibco Co. (Gibco BRL, Rockville, MD; NY). 5-(and-6)-Chloromethyl-2′,7′-dichlorodihydrofluorescein diacetate, acetyl ester (CM-H_2DCFDA), dihydroethidium, Bapta-acetoxymethyl (AM), and Indo-1 were supplied from Molecular Probes (Eugene, OR). Pifithrin-α (PFT-α), SP600125, and SOD were purchased from Calbiochem (San Diego, CA).

Cell culture and treatment. The JB6 P^+ mouse epidermal cell line, Cl41 (JB6 Cl41 cells; ATCC, Manassas, VA, CRL-2010), and cells stably transfected with the activator protein 1 (AP-1)-luciferase reporter plasmid (JB6/AP-1 cells) were cultured in EMEM supplemented with 5% FBS, 2mM L-glutamine, and 50 μg of gentamicin/ml. The cells were grown at 37°C in a 5% CO_2 atmosphere. One million cells per milliliter were resuspended in the growth medium and divided into 60-mm culture dishes or 96-well plates. When the cells reached 80% confluence, the medium was replaced with fresh EMEM containing 0.5% FBS and various concentrations of $CdCl_2$ (0–10μM).

Measurement of cell viability and cytotoxicity. 3-(4,5-Dimethylthiazol-2yl-)-2,5-diphenyl tetrazolium bromide (MTT) was used to evaluate the cell viability. JB6 Cl41 cells were cultured in EMEM supplemented with 0.5% FBS in the presence of 0–10μM of $CdCl_2$ for 24 h. For inhibition assays, CAT (500 U/ml), SOD (500 U/ml), Bapta-AM (0–10μM), PFT-α (0–10μM), and SP600125 (0–20μM) were added into the cultures in the presence of 10μM cadmium. After 24-h incubation, 5 μl of a MTT solution (5 mg/ml in PBS as stock solution) was added into each well of 96-well plate and incubated for another 4 h at 37°C. MTT-reducing activity of cells was measured by treating them with acidic isopropanol prior to reading at 570 nm with a Spectra Max Plus^{384} spectrometer (Molecular Devices, Sunnyvale, CA). In addition, cytotoxicity was measured using a trypan blue exclusion assay. In brief, cells were stained with 0.4% trypan blue, and ~100 cells were counted for each treatment. The cytotoxicity was calculated as follows: % cytotoxicity = ([total cells − viable cells]/total cells) × 100%.

Fluorescein isothiocyanate-Annexin V/propidium iodide staining. JB6 Cl41 cells were washed twice with PBS before being suspended in 1× binding buffer (10mM 4-(2-hydroxyethyl)-1-piperazineethanesulfonic acid (Hepes) pH 7.4, 140mM NaOH, and 2.5mM $CaCl_2$). Five microliters of fluorescein isothiocyanate (FITC)-labeled Annexin V was mixed with 100 μl of cell suspensions containing 1×10^5 cells, and the cells were incubated at room temperature for 5 min. Thereafter, 2 μl of propidium iodide (PI) solution (10 μg/ml) was added to the cells, followed by an additional 5-min incubation. The scatter parameters of the cells (20,000 cells per experiment) were analyzed using a FACS Calibur system (BD, Franklin Lakes, NJ). Four cell populations were identified according to the following interpretation: viable population in the lower-left quadrant (low-PI and FITC signals), early apoptotic population in the lower-right quadrant (low-PI and high-FITC signals), necrotic population in the upper-left quadrant (high-PI and low-FITC signals), and late apoptotic or necrotic population in the upper-right quadrant (high-PI and high-FITC signals).

Agarose gel electrophoresis. Cells were incubated with a lysis buffer (1% nonidet P-40 (NP-40) and 1% SDS in 50mM Tris-HCl, pH 8.0) at 65°C for 1 h. DNA was extracted with phenol/chloroform/isoamyl alcohol, and the aqueous phase was precipitated overnight with two volumes of absolute ethanol at −20°C. The pellet was air-dried and resuspended in TE buffer (10mM Tris-Cl and 1mM EDTA, pH 8.0). The degree of fragmentation was analyzed using 2% agarose gel electrophoresis, followed by ethidium bromide staining.

Western blot analyses. Cell lysates were made in a lysis buffer (50mM Tris-Cl, pH 7.4; 1mM EDTA; 150mM NaCl; 1% NP-40; 0.25% Na-deoxycholate; and 1 μg/ml of aprotinin, leupeptin, and pepstatin). Equal amounts (20 μg/sample) of protein were separated by the NuPAGE Bis-Tris electrophoresis system (Invitrogen, Carlsbad, CA) and blotted onto a nitrocellulose membrane (Whatman, Dassel, Germany). Blots were probed with primary antibodies for either 2 h at room temperature or overnight at 4°C before incubation with horseradish peroxidase–conjugated anti-IgG in blocking buffer for 1 h. Polyclonal antibody specific to apoptosis inducing factor (AIF) (SC-5586) and monoclonal antibodies specific for cytochrome c (SC-13156), GADD45α (SC-797), β-actin (SC-47778), and p-c-Jun-NH_2-terminal kinase (p-JNK) (SC-6252) were purchased from Santa Cruz Biotechnology (Santa Cruz, CA). The monoclonal antibodies specific to Bcl-2 (M0887) and caspase-8 (804-242-C100) were from Dakocytomation (Glostrup, Denmark) and ALEXIS (San Diego, CA), respectively. Bcl-xL (2762), Bcl-2 (2876), EndoG (4969), COX IV (4850), p-p53 (Ser 15) (9284), c-Jun (9162), p-c-Jun (9261), JNK (9252), cleaved caspase-9 (Asp 315) (9595), cleaved caspase-3 (Asp 175) (9661), and cleaved caspase-7 (Asp 198) (9491) polyclonal antibodies were purchased from Cell Signaling (Beverly, MA). The monoclonal antibodies specific to p53 (OP03) and Smac/Diablo (612245) were purchased from Oncogene (La Jolla, CA) and BD Biosciences (San Jose, CA) (Pharmingen), respectively. Secondary antibodies and enhanced chemiluminescence substrate were from Pierce (Rockford, IL). The blots were exposed to Hyperfilm (Amersham Pharmacia Biotech, Piscataway, NJ), and bands were quantified with ImageJ densitometry software (NIH, Bethesda, MD).

Preparation of cellular fractions. JB6 Cl41 cells were washed with PBS and resuspended for 20 min in an ice-cold lysis buffer (250mM sucrose; 20mM Hepes, pH 7.5; 10mM KCl; 1.5mM $MgCl_2$; 1mM each of ethylene glycol tetraacetic acid, EDTA, dithiothreitol (DTT), and phenylmethanesulphonyl-fluoride (PMSF); and 10 μg/ml each of leupeptin, aprotinin, and pepstatin A). The cells were centrifuged at 750 × g for 10 min at 4°C, and the supernatants were further centrifuged at 10,000 × g for 25 min at 4°C in order to prepare the cytosolic fraction. The remaining pellets were resuspended in the lysis buffer and used as the mitochondrial fraction after centrifugation at 10,000 × g for 25 min. For nuclear proteins extracts, cells were resuspended with buffer A (20mM Hepes, pH 7.9; 10mM NaCl; 3mM $MgCl_2$; 0.1% NP-40; 10% glycerol; 0.2mM EDTA; 1mM DTT; 0.4mM PMSF; and 1 μg/ml each of leupeptin, aprotinin, and pepstatin A). After centrifugation at 1000 × g for 5 min, the pellets were washed with 125 μl of buffer B (20mM Hepes, pH 7.9; 20% glycerol; 0.2mM EDTA; 1mM DTT; 0.4mM PMSF; and 1 μg/ml each of leupeptin, aprotinin, and pepstatin A) and dissolved with 50 μl buffer C (20mM Hepes, pH 7.9; 400mM NaCl; 3mM $MgCl_2$; 20% glycerol; 0.2mM EDTA; 1mM DTT; 0.4mM PMSF; and 1 μg/ml each of leupeptin, aprotinin, and pepstatin A). The extracts were centrifuged at 10,000 × g for 25 min, and the supernatants were used as the nuclear fractions.

Determination of caspase activity. The activity of caspases was assessed using the luminescent Caspase-Glo 3/7 assay system (Promega, Madison, WI) according to the manufacturer's instructions. Briefly, cells were treated with various concentrations of $CdCl_2$ (0–10μM) for 24 h and then 100 μl of Caspase-Glo 3/7 Reagent was added into each well of 96-multiwell plates. After 1-h incubation at room temperature, the luminescence was measured using Glomax 96 microplate luminometer (Promega).

Measurement of cellular hydrogen peroxide (H_2O_2) and superoxide anion ($O_2^{\cdot-}$) production. Dihydroethidium and CM-H_2DCFDA are specific dyes used for staining $O_2^{\cdot-}$ and H_2O_2, respectively, which are produced by intact cells (Qian *et al*., 2003; Zamzami *et al*., 1995). JB6 Cl41 cells (2×10^4 cells) were seeded onto a glass coverslide in the bottom of a 24-well plate for overnight. The cells were exposed to $CdCl_2$ (0–10μM) for 12 h and then dihydroethidium (5μM) or CM-H_2DCFDA (5μM) was added into the cells for 30 min. Cells were washed with PBS, mounted, and observed under an inverted Leica IRBE confocal microscope (Leica, Wetzlar, Germany). In addition, JB6 Cl41 cells (0.5×10^6 cells per well) were seeded into 60-mm culture dishes, and after overnight incubation, the cultures were treated with $CdCl_2$ (0–10μM) and/or CAT (500 U/ml) for 12 h. Finally, the cells were exposed to either dihydroethidium or CM-H_2DCFDA at the final concentration of 5μM for 30 min and processed for flow cytometric analysis.

Measurement of intracellular calcium. Intracellular calcium was measured with probe Indo-1/AM (cell permeates). JB6 Cl41 cells were incubated in

EMEM containing $CdCl_2$ (0–10μM) and/or Bapta-AM (0–10μM) at 37°C for 12 h, and the medium was replaced with a fresh EMEM supplemented with Indo-1 (1μM), followed by additional 30-min incubation. Cells were washed twice with PBS to remove the intracellular AM esters before being analyzed using a flow cytometer. Emissions of Indo-1 specific for free Ca^{2+} and bound Ca^{2+} were detected using 530/30-nm filter and 405/30-nm filter, respectively, where the signals were separated by a 470-nm long-pass dichroic filter.

Assay of AP-1 activity. When JB6/AP-1 cells reached 80–90% confluence, the cells were incubated in a low serum (0.5% FBS) containing EMEM for 24 h to minimize basal AP-1 activity. The cells were exposed to various concentrations of $CdCl_2$ (0–10μM) for 24 h, and luciferase activity specific to AP-1 was then measured by using a luciferase assay kit (Promega) as described elsewhere (Ding *et al*., 1999). The results were expressed as relative AP-1 activity compared with control.

Small interference RNA transfection. Silencer predesigned small interference RNA (si-RNA) for mouse *AIF* (si-RNA ID: S77394), *EndoG* (si-RNA ID: S201290), *JNK1* (si-RNA ID: 188653), *JNK2* (si-RNA ID: 73119), *p53* (si-RNA ID: 187425), and control *GAPDH* (si-RNA ID: 4390849) were obtained from Ambion (Austin, TX). Skin epidermal cells were seeded in 96- or 6-well culture plates and transfected at ~50% confluency with the si-RNA duplexes using Lipofectamine RNAi MAX (Invitrogen) according to the manufacturer's instructions. Medium was changed after 6 h to minimize cytotoxicity. Cellular levels of the proteins specific for the si-RNA transfection were checked by immunoblotting, and all experiments were performed 24 h after transfection.

Statistical analysis. All the data are expressed as mean ± SE. One-way ANOVA using SPSS ver. 10.0 software was used for multiple comparisons. A value of $p < 0.05$ was considered statistically significant.

RESULTS

Cadmium Induces Cell Death Mainly by Apoptosis in Skin Epidermal Cells in a Dose-Dependent Manner

Cadmium induced a dose-dependent cytotoxic effect on skin epidermal cells as expected. Treating the cells with 5 and 10μM cadmium for 24 h decreased the MTT-reducing activity to 80.2 and 51.5%, respectively, relative to untreated control cells (Fig. 1A). In addition, cadmium significantly increased the number of trypan blue–positive cells such that ~45% of cells were positive to the dye when exposed to 10μM cadmium for 24 h (Fig. 1B). There was no observable cytotoxicity of cells under exposure to 1μM cadmium. Cadmium treatment also caused cell death in a time-dependent manner from 1 to 24 h (data not shown). Cadmium-induced toxicity was supported by optic microscopic observation, which showed an increase in cell shrinkage depending on the dose of cadmium (Fig. 1C).

The results from fluorescence staining and agarose gel electrophoresis revealed that cadmium-induced cytotoxicity was due to apoptosis. Cadmium treatment increased early and late apoptotic population in a dose-dependent manner (Fig. 1D). Approximately 8% of cell population expressing high-PI and low-FITC signals, which corresponds with necrotic cells, was observed when the cells were exposed to 10μM cadmium. Under the same conditions, more than 23% of cell populations were determined to be apoptotic (Fig. 1E). Exposure of the cells to cadmium also led to a cleared ladder formation of genomic DNA, and the DNA fragmentation was quite prominent in cells exposed to 10μM cadmium (Fig. 1F). These results suggest that cadmium predominantly not only causes apoptosis in skin epidermal cells but also leads to necrotic cell death depending on the exposed dose.

Cadmium-Induced Apoptosis Is Mediated by a Caspase-Independent Pathway

Figure 2A shows that cadmium treatment resulted in the induction of a cleaved caspase-8 band and the decrease of cellular Bid, Bcl-xL, and Bcl-2 levels. However, there were no cleaved forms corresponding to caspase-3, -7, and -9, suggesting that cadmium-induced apoptosis is caspase

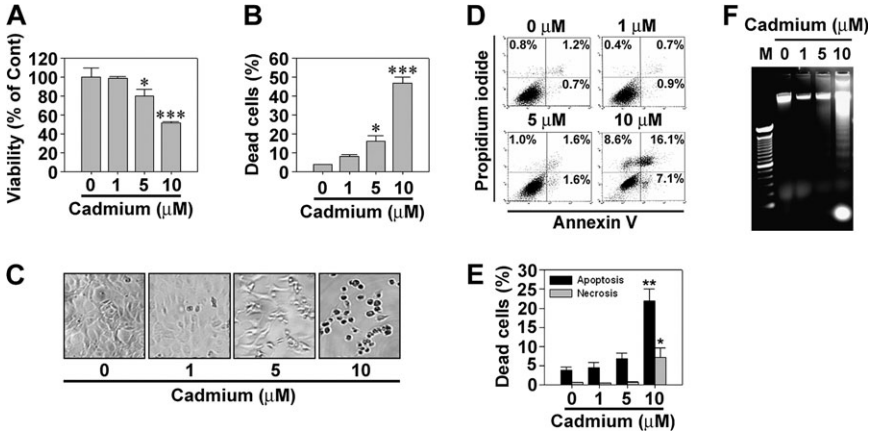

FIG. 1. Cadmium induces cytotoxicity by apoptosis in skin epidermal cells in a dose-dependent manner. The cells were exposed to increasing concentrations (0–10μM) of cadmium for 24 h and then processed for (A) MTT assay, (B) trypan blue staining, (C) optic microscopic observation, (D and E) flow cytometric analysis after Annexin V and PI staining, and (F) agarose gel electrophoresis. The results are shown as the mean ± SE of three separate experiments. *$p < 0.05$, **$p < 0.01$, and ***$p < 0.001$ versus the untreated control values (ANOVA, Scheffe's test). In panel E, the percentage of apoptotic populations was summed up from the early apoptotic cells (annexin V^+/PI^-) and late apoptotic cells (annexin V^+/PI^+) from triplicate experiments. In panel F, M means DNA size marker.

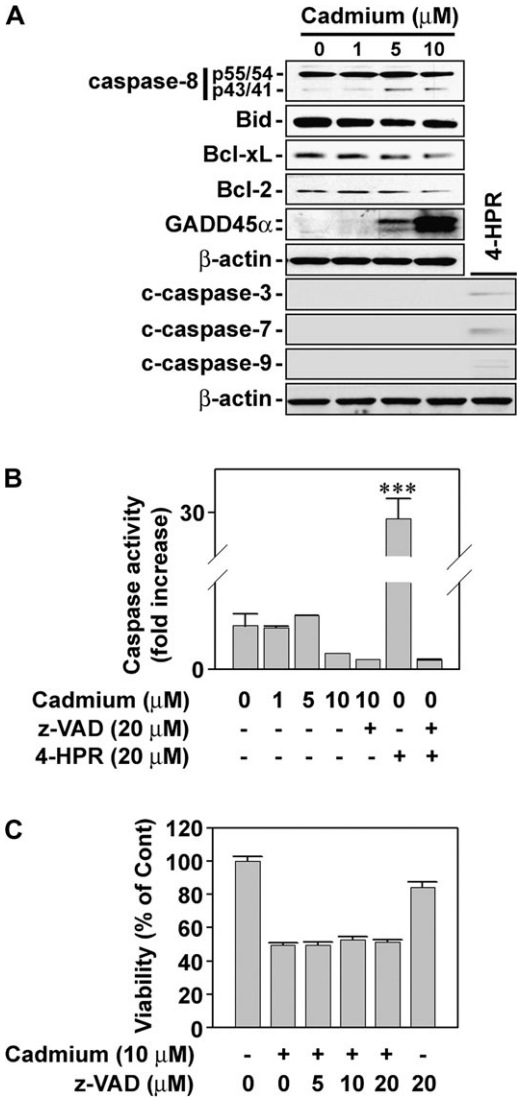

FIG. 2. Cadmium induces apoptosis by a caspase-independent manner. (A) Cellular proteins were prepared from the cells exposed to the indicated concentrations of cadmium for 24 h and then processed for Western blot analysis. A representative result from triplicate experiments is shown. Skin epidermal cells were exposed to cadmium in the presence of pancaspase inhibitor, z-VAD fmk (20μM), or N-(4-hydroxyphenyl) retinamide (4-HPR; 20μM) for 24 h and adjusted to the analyses for caspase activity (B) and cell viability by MTT assay (C). The results represent the mean ± SE of three independent experiments. ***$p < 0.001$ versus the untreated control value. In this assay, 4-HPR was used as a caspase-dependent positive control.

independent. This conclusion was supported by the observation that the activity of caspase-3/7 was not changed by treating the cells with cadmium, whereas N-(4-hydroxyphenyl) retinamide (4HPR)–mediated activation of caspases was completely inhibited by a pancaspase inhibitor, benzyloxycarbonyl-Val-Ala-Asp (OMe) fluoromethylketone (z-VAD fmk) (Fig. 2B). In addition, the cadmium-induced decrease in cell viability was not prevented even though 20μM z-VAD fmk was added into the cells (Fig. 2C).

Cadmium-Induced Apoptosis Is in Part Related to AIF-Mediated Signaling

We next examined whether mitochondrial-mediated signaling is involved in cadmium-induced cell death. Western blot analysis showed that mitochondrial death effectors, such as AIF, EndoG, cytochrome c, and Smac/Diablo, were released from the mitochondria into the cytosol by exposing cells to cadmium in a dose-dependent manner (Fig. 3A). Cadmium treatment also induced the nuclear translocation of AIF and EndoG from the mitochondria (Fig. 3B). However, Bax translocation to the mitochondria from the cytosol was not shown in this experiment (Fig. 3A). In addition, cadmium decreased $\Delta\Psi m$ when the skin epidermal cells were flow cytometrically analyzed after staining with JC-1, a cationic mitochondrial-specific fluorescent dye (data not shown). These results led us to hypothesize that mitochondrial stress is closely associated with cadmium-mediated apoptosis of skin epidermal cells, where both AIF and EndoG play important roles. For further verification, we transfected the cells with si-RNAs specific to AIF or EndoG by which the expression of both proteins was clearly attenuated (Fig. 3C). However, the cadmium-induced decrease in cell viability was attenuated only in the cells transfected with si-AIF (Fig. 3D). These findings suggest that AIF is one of the mediators in cadmium-induced apoptosis in this study.

Intracellular Production of Hydrogen Peroxide Is the Important Event in Cadmium-Induced Cell Death

To investigate whether intracellular ROS is involved in cadmium-induced cell death, skin epidermal cells were stained with either CM-H_2DCFDA or dihydroethidium. Flow cytometry analysis showed that the fluorescence intensity of DCF signal, corresponding to the H_2O_2 content, was right shifted after treatment with cadmium in a dose-dependent manner (Fig. 4A, upper-left panel). This shift was inhibited by adding CAT to the cultures (Fig. 4A, upper-right panel), indicating that cadmium leads to the generation of intracellular H_2O_2 in JB6 Cl41 cells. Similarly, the fluorescence intensity specific for H_2O_2 was higher in the cadmium-exposed cells than in the untreated control cells (Fig. 4A, bottom panel). In contrast, the fluorescence intensity of dihydroethidium, which is specific for $O_2^{\cdot-}$, was not significantly changed by cadmium, as shown in the data from flow cytometric (Fig. 4B, upper panel) and fluorescence microscopic analyses (Fig. 4B, bottom panel). Cadmium-induced decrease in cell viability was significantly inhibited by adding CAT, but not SOD, into the cultures (Fig. 4C). In fact, SOD further decreased the cell viability. This decrease is likely due to an increase in H_2O_2 content because dismutation of $O_2^{\cdot-}$ catalyzed by SOD generates H_2O_2. These results demonstrate that H_2O_2, but not $O_2^{\cdot-}$, plays an important role in mediating apoptosis in cadmium-exposed cells.

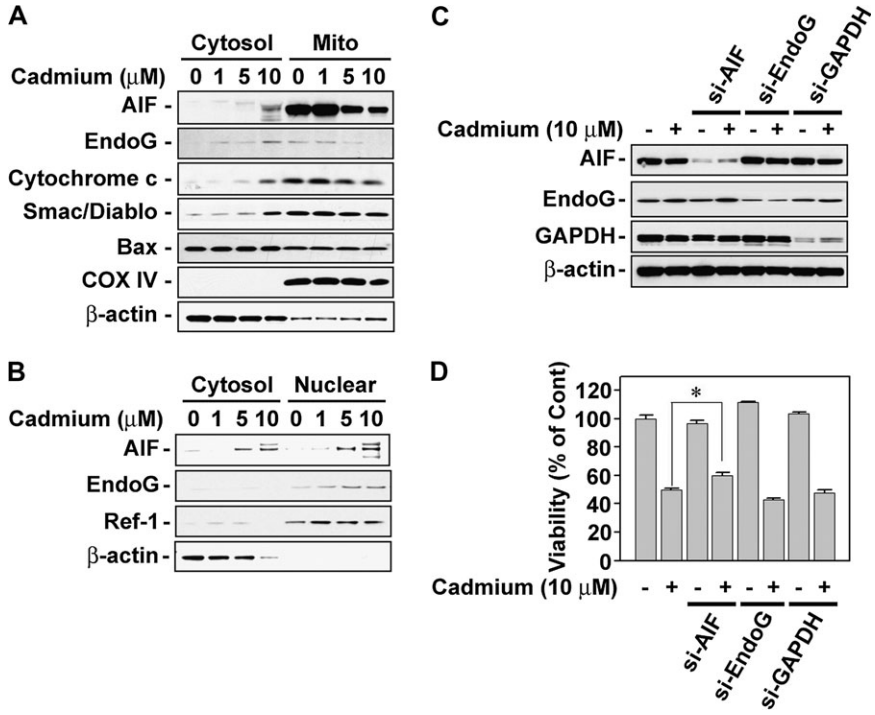

FIG. 3. Nuclear translocation of AIF from the mitochondria participated in the cadmium-induced decrease of cell viability. (A and B) Cell fractions (cytosolic, mitochondrial, and nuclear) were prepared from the cells subjected to the various doses (0–10μM) of cadmium for 24 h and then analyzed by NuPAGE Bis-Tris electrophoresis system, followed by immunoblot analysis. In addition, skin epidermal cells were transfected with si-RNA specific for AIF, EndoG, and GAPDH, and they were exposed to 10μM cadmium. At 24-h incubation, the expression levels of these proteins and viability of the cells were analyzed by Western blot assay (C) and MTT assay (D), respectively. Cytochrome c oxidase IV (COX IV) and Ref-1 were used as the internal markers specific to mitochondria and nucleus, respectively. β-Actin was used as loading control. *$p < 0.05$ represents significant difference between the experiments.

Cadmium also Induces Calcium-Dependent Cell Death in Skin Epidermal Cells

It has been reported that intracellular calcium signaling is involved in cadmium-induced apoptosis in various cell types (Kim and Sharma, 2004; Lee *et al*., 2006; Lemarie *et al*., 2004; Li *et al*., 2000; Shih *et al*., 2005; Wang *et al*., 2008). Consistent with these reports, flow cytometric analysis showed that exposure of JB6 Cl41 cells to cadmium for 12 h triggered an

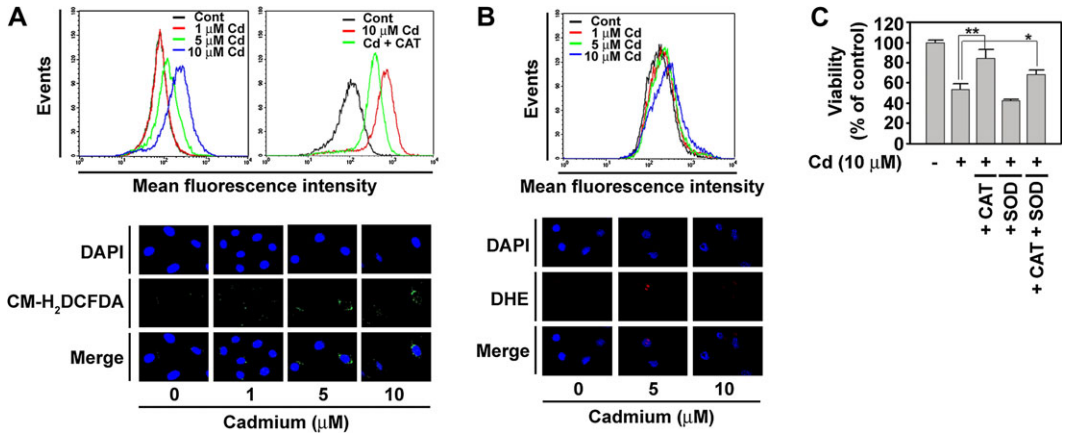

FIG. 4. Cadmium causes cell death through the generation of hydrogen peroxide in skin epidermal cells. Cells were incubated with various cadmium concentrations (0–10μM) in the presence or absence of 500 U/ml CAT for 12 h. (A) The cells were analyzed by flow cytometry after treatment with 5μM CM-H_2DCFDA for 30 min (upper panels) or by fluorescence microscopy (magnification ×200) after the fluorescent treatment followed being counterstained with 2μM 4',6-diamidino-2-phenylindole (DAPI) (bottom panel). (B) The cells were also incubated with the indicated concentrations of cadmium for 12 h before treating with 5μM dihydroethidium for 30 min and processed for flow cytometric (upper panel) and fluorescence microscopic analyses (bottom panel). (C) In addition, the cells were incubated with 10μM cadmium in the presence of CAT or SOD for 24 h and then MTT assay was carried out. *$p < 0.05$ and **$p < 0.01$ versus the cadmium treatment alone.

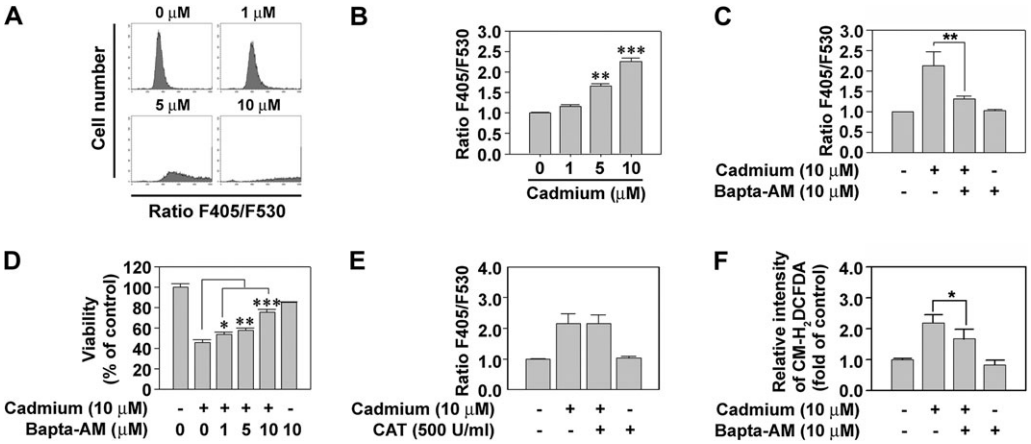

FIG. 5. Intracellular-free calcium ions are also critical for the induction of cell death in cadmium-exposed cells. (A) Skin epidermal cells were exposed to the indicated concentrations (0–10μM) of cadmium for 12 h and then they were treated with 1μM Indo-1 for 30 min before flow cytometric analysis. (B) The F_{405}/F_{530} ratio of Indo-1 was calculated from triplicate experiments. $^{**}p < 0.01$ and $^{***}p < 0.001$ versus the untreated control value. In addition, the cells were incubated in the medium containing 10μM cadmium, 1μM Indo-1, and/or various concentrations (0–10μM) of Bapta-AM and then processed for the analyses of the F_{405}/F_{530} ratio of Indo-1 (C), cell viability using MTT assay (D), and the fluorescence intensity of CM-H_2DCFDA (F). In the experiment of E, the cells were exposed to 10μM cadmium with and without 500 U/ml CAT and then the F_{405}/F_{530} ratio of Indo-1 was determined as described in the ''Materials and Methods'' section. Results are shown as the mean ± SE of at least three independent experiments. $^{*}p < 0.05$, $^{**}p < 0.01$, and $^{***}p < 0.001$ versus the cadmium treatment alone.

increase in cytoplasmic free calcium in a concentration-dependent manner (Fig. 5A). Intracellular calcium levels were increased by 1.66- and 2.26-fold upon the addition of 5 and 10μM cadmium, respectively, compared with the untreated control (Fig. 5B). Treatment of cells with Bapta-AM (10μM), an intracellular-free calcium chelator, diminished the cadmium-mediated elevation in intracellular calcium level (Fig. 5C). Moreover, the addition of Bapta-AM into cadmium-exposed skin epidermal cells blocked the metal-induced reduction of cell viability in a dose-dependent manner; cell viability was observed to be 57.9 and 75.2% at 5 and 10μM Bapta-AM treatment, respectively, compared with 45.6% without Bapta-AM treatment (Fig. 5D).

We subsequently investigated whether there is a relationship between calcium release and hydrogen peroxide production in cadmium-exposed skin epidermal cells. CAT treatment did not suppress the cadmium-stimulated calcium flux in the cells (Fig. 5E), whereas Bapta-AM significantly reduced the cadmium-stimulated DCF intensity (Fig. 5F). The results demonstrate that cadmium increases intracellular calcium level, which mediates the generation of H_2O_2 in skin epidermal cells.

p53 and JNK Signaling Plays Important Roles in the Cadmium-Induced Cell Death of Skin Epidermal Cells

Since p53- and JNK-mediated pathways have critical roles in apoptosis induced by a variety of stresses, such as ROS, irradiation, and toxic chemicals, we determined the levels of p-p53 and p-JNK in cadmium-exposed skin epidermal cells. Treating the cells with cadmium increased the level of p-p53 in a dose-dependent manner (Fig. 6A). The levels of p-JNK1 (p46) and p-JNK2 (p54) were also augmented by exposing the cells to cadmium (Fig. 6B). When skin epidermal cells were treated with various doses of PFT-α (0–10μM) or SP600125 (0–20μM) in the presence of cadmium (10μM), both inhibitors prevented the cadmium-mediated decrease of cell viability in a dose-dependent manner (Figs. 6C and 6D). These results indicate that p53- and JNK-mediated signalings have crucial roles in cadmium-induced cell death in skin epidermal cells.

Because JNK affects AP-1-DNA-binding activation, we examined whether cadmium is able to stimulate c-Jun phosphorylation and AP-1 activation using skin epidermal cells transfected with an AP-1-luciferase reporter plasmid (Li *et al.*, 1997). Cellular levels of c-Jun and p-c-Jun were augmented by treating the cells with cadmium in a dose-dependent manner. When the cells were exposed to 10μM cadmium, the levels of c-Jun and p-c-Jun were 6.73- and 26.24-fold higher than that of the untreated control cells, respectively (Fig. 6E). Cadmium treatment also dramatically increased the luciferase activity specific for AP-1 in the cells, suggesting the involvement of AP-1–mediated signaling in cellular responses to cadmium (Fig. 6F).

Cadmium Activates the JNK- and p53-Mediated Pathways through the Induction of Calcium Ion and H_2O_2, Respectively, in Skin Epidermal Cells

To further understand the signal transduction pathways involved in cadmium-induced cell death, skin epidermal cells were exposed to 10μM cadmium in the presence of CAT or pharmacological inhibitors specific for calcium-free ion, p53, and JNK, followed by Western blot analysis. Treating the cells with CAT (500 U/ml) decreased the cadmium-induced elevations of levels of p-p53, p-c-Jun, and c-Jun (Fig. 7A). Cellular levels of p-JNK1/2 or GADD45α were not affected by the addition of CAT to the cells. In contrast, exposure of cells

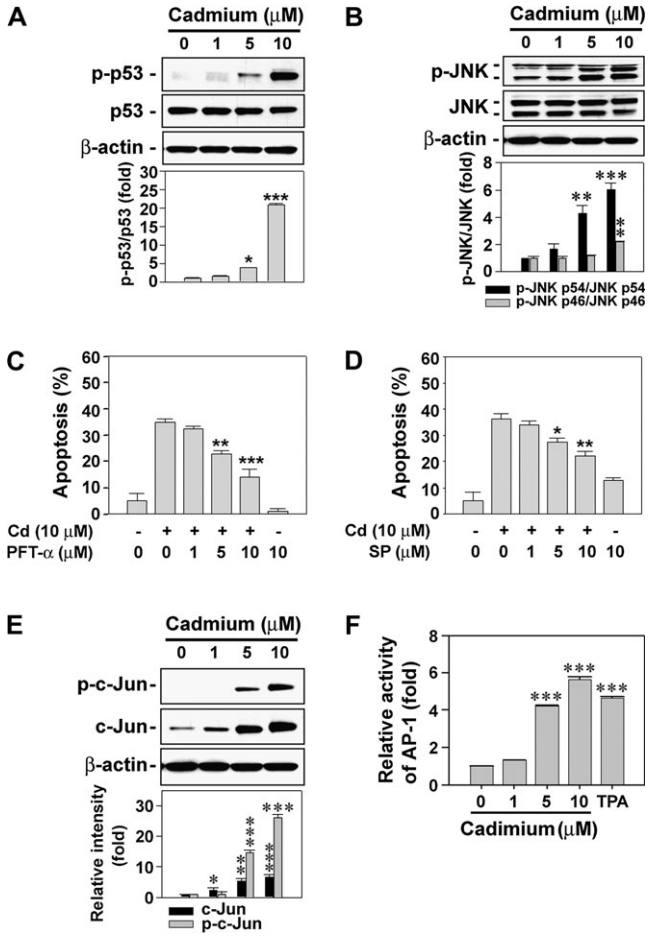

FIG. 6. p53- and JNK-mediated signaling plays critical roles in cadmium-induced apoptosis in skin epidermal cells. The cells were incubated with various concentrations (0–10μM) of cadmium for 24 h and then analyzed by immunoblotting using p53- (A) or JNK-specific antibodies (B). The data were quantified through densitometry, and the band intensities are expressed as the mean ± SE relative to the control after normalizing the bands to total p53 and JNKs, respectively. The cells were also exposed to 10μM cadmium with the indicated concentrations (0–10μM) of p53 inhibitor, PFT-α (C), or JNK inhibitor, SP600125 (D), for 24 h. Apoptosis was determined by Annexin V and PI staining, and the results are shown as the mean ± SE of three separate experiments. $*p < 0.05$, $**p < 0.01$, and $***p < 0.001$ versus the cadmium treatment alone. In addition, JB6 cells transfected with AP-1 promoter gene were exposed to the indicated concentrations (0–10μM) of cadmium in the presence and absence of 20 ng/ml 12-*O*-tetradecanoylphorbol-13-acetate. After 24-h incubation, the cells were processed for the analyses of c-Jun expression by Western blot analysis (E) or the AP-1 activity by luciferase assay, presented as relative AP-1 induction compared with the untreated control cells (F). In the experiment of E, a representative data were shown, and the intensity of bands is expressed as the mean ± SE relative to the control of triplicate experiments after normalizing the bands to β-actin. $*p < 0.05$, $**p < 0.01$, and $***p < 0.001$ versus the unexposed control values.

to 10μM Bapta-AM inhibited the phosphorylation of JNK1 and JNK2 in cadmium-exposed cells, whereas it accelerated the cadmium-mediated increase of p-p53 and p-c-Jun levels in the cells (Fig. 7B). In the case of GADD45α, the cadmium-stimulated expression was almost completely suppressed by the Bapta-AM treatment. These results suggested that the activation of p53- and c-Jun–mediated signaling in cadmium-exposed cells is related to H_2O_2 generated by the metal. It is also believed that JNK- and GADD45α-mediated pathways are upregulated by intracellular calcium ions in cadmium-exposed skin epidermal cells. Further experiments revealed that a p53-specific inhibitor, PFT-α, inhibited p53 phosphorylation rather than expression and blocked the cadmium-mediated reduction of cellular Bcl-2 and Bcl-xL levels, indicating involvement of p53-mediated signaling in cadmium-induced mitochondrial stress (Fig. 7C). PFT-α treatment did not affect the levels of p-c-Jun, c-Jun, and GADD45α that had stimulated in cadmium-treated cells. However, the JNK-specific inhibitor, SP600125, dramatically blocked the cadmium-mediated increases of p-c-Jun, c-Jun, and GADD45α levels but not of Bcl-2 and Bcl-xL in the cells (Fig. 7D). These findings clarify the important roles of JNK in upregulating the expression of GADD45α and c-Jun.

Blockage of JNK and p53 by Transfection of Their Specific si-RNAs Inhibits the Cadmium-Induced Apoptosis in Skin Epidermal Cells

We examined the precise roles of JNK- and p53-mediated signaling in cadmium-induced cell death by inhibiting their expressions *via* si-RNA transfection. Transfecting the cells with JNK1-specific si-RNA attenuated the expression of GADD45α in the cells exposed to 10μM cadmium (Fig. 8A), while transfection with JNK2-specific si-RNA completely blocked GADD45α expression. The inhibition of GADD45α by the si-JNKs resulted in the significant protection of the cells against cadmium-induced toxic effect, where the viability and apoptosis transfected with si-JNK2 were more effective than that with si-JNK1 (Figs. 8B–D). These results verify that GADD45α plays a critical role in mediating cadmium-induced toxicity in skin epidermal cells, which is regulated by JNK2-mediated signaling. Similar to the case of PFT-α treatment, the inhibition of p53 by its si-RNA transfection attenuated decreased the cellular levels of Bcl-2 and Bcl-xL with the concomitant increase of cell viability that was reduced by cadmium treatment (Fig. 8B). Furthermore, transfecting the cells with si-RNA specific to p53 attenuated cytotoxicity and apoptosis in cadmium-exposed cells (Figs. 8B–D). However, necrosis was not affected by transfection of si-RNA specific to JNK1/2 or p53 in cadmium-exposed skin epidermal cells (Figs. 8C and D).

DISCUSSION

Cadmium affects a diverse range of cellular events, such as proliferation, differentiation, and apoptosis. Whereas the cytotoxic and carcinogenic roles of cadmium in the lung, liver, and kidney have been extensively studied, only limited studies are available for skin. The present study demonstrates

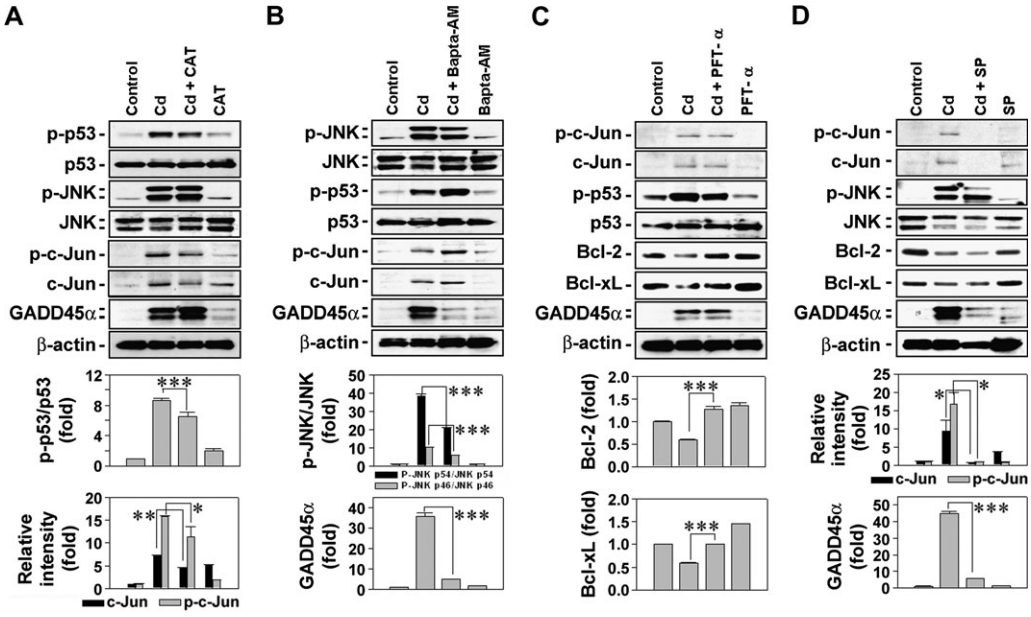

FIG. 7. Determination of signaling pathways involved in the p53- and JNK-mediated apoptosis of cadmium-exposed cells. Skin epidermal cells were exposed to 10μM cadmium in the presence of various types of chemical inhibitors, such as CAT (500 U/ml) (A), Bapta-AM (10μM) (B), PFT-α (10μM) (C), and SP600125 (20μM) (D). After 24-h exposure, cellular proteins were prepared from the cells and analyzed by Western blot assay. A representative data from triplicate experiments were shown, and the band intensities are calculated using densitometer being expressed as the mean ± SE relative to the control after normalizing the bands to total protein or β-actin. $*p < 0.05$, $**p < 0.01$, and $***p < 0.001$ represent significant differences between the experiments.

that cadmium induces cell death mainly by caspase-independent apoptosis through the activation of JNK- and p53-mediated signaling in skin epidermal cells, with H_2O_2 and calcium ions acting as pivotal mediators of the signaling.

Our current findings show that cadmium causes cytotoxicity on skin epidermal cells in a dose-dependent manner, where ~50% of cells were killed by treating 10μM for 24 h. This cytotoxic level is similar to that observed when mesangial and

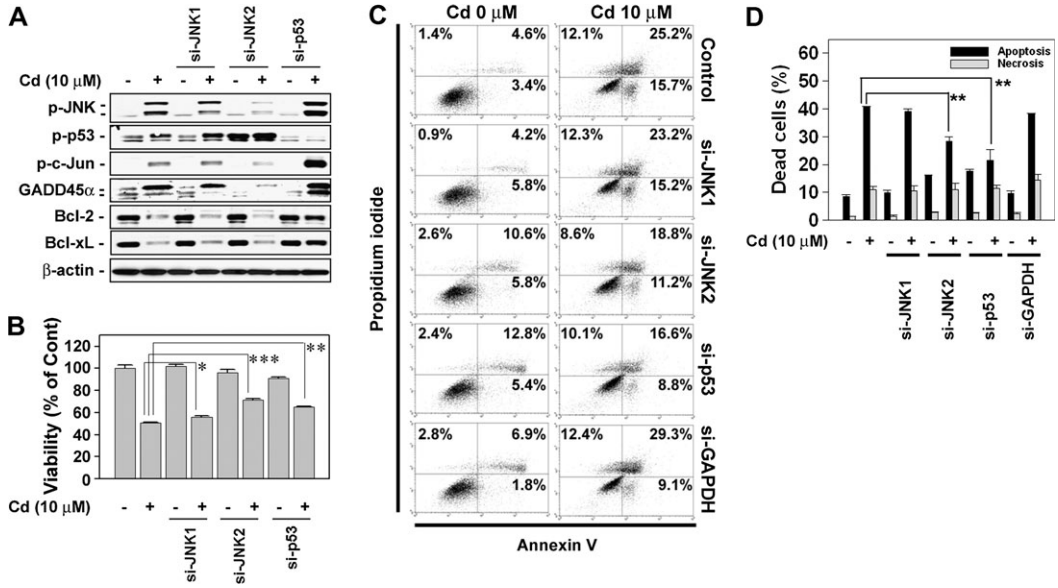

FIG. 8. Transfecting cells with si-JNKs or si-p53 prevent cadmium-induced apoptosis. Skin epidermal cells were transfected with si-RNAs specific to JNK1, JNK2, and p53. Following 24-h incubation, they were exposed to 10μM cadmium for additional 24 h. Finally, the cells were analyzed by Western blotting (A), MTT assay (B), and apoptosis assay (C and D). The results are shown as the mean ± SE of three separate experiments. $*p < 0.05$, $**p < 0.01$, and $***p < 0.001$ versus the cadmium treatment alone. In panel D, the percentage of apoptotic populations was summed up from the early apoptotic cells (annexin V^+/PI^-) and late apoptotic cells (annexin V^+/PI^+) from triplicate experiments.

human hepatoma cells were treated with the same conditions (Lemarie *et al*., 2004; Wang *et al*., 2008) but is much higher than that seen in rat lung epithelial cells (Gong and Hart, 1997). In parallel with the previous *in vitro* and *in vivo* studies (Hewison *et al*., 1996; Xu *et al*., 1996), cadmium induces cell death by apoptosis in skin epidermal cells, as proven by the appearance of cell shrinkage, the formation of nuclear DNA ladders, and the increase of Annexin V–positive stained cells.

Cadmium-induced toxicity can engage both caspase-dependent and-independent (Hossain *et al*., 2009; Mao *et al*., 2007; Wang *et al*., 2009). It is likely that cadmium induces apoptosis *via* a caspase-independent pathway in skin epidermal cells. This is because there were no increases in the activated forms of caspase-3, -7, and -9, although caspase-8 appeared to be activated in the cadmium-treated cells. In addition, pancaspase inhibitors did not affect the levels of caspase-3/7 activity or the viability in cadmium-exposed cells. Furthermore, the cleavage of poly (ADP-ribose) polymerase, which is mediated by the activation of executive caspases (Yakovlev *et al*., 2000), is not observed in cadmium-exposed cells (data not shown). It is worth considering that caspase-8 stimulates both caspase-dependent and -independent pathways by converting Bid to tBid (Yin *et al*., 1999). In the caspase-independent induction of apoptosis, AIF and EndoG are believed to exert critical roles, where they are relocated into the nuclei from the mitochondria, thereby inducing chromatin condensation and large-scale DNA fragmentation (Susin *et al*., 1999). This study shows that cadmium stimulated the release of the death effecters from the mitochondria in skin epidermal cells. Knockout of AIF by si-RNA transfection attenuates the cadmium-induced toxicity in the cells, whereas blocking EndoG does not show any protective effect. This finding implies that AIF is related to cadmium-induced apoptosis in the cells.

Cadmium reduces the cellular levels of Bcl-2 and Bcl-xL, but not of Bax, in skin epidermal cells in a dose-dependent manner. This means that cadmium-induced apoptosis involves mitochondrial stress through the downregulation of antiapoptotic factors. It has been shown that the tumor suppressor p53 acts as the upstream effecter of Bcl-2 family proteins (Galluzzi *et al*., 2008) and an important regulator for apoptosis induced by ROS (Polyak *et al*., 1997). A notable result of this study is that blockage of p53 expression with a pharmacological inhibitor or si-RNA transfection significantly prevents cadmium-induced cytotoxicity with the attendant increase of Bcl-2 and Bcl-xL expression. These results verify that p53-Bcl-2/Bcl-xL–mediated signaling is required for the apoptosis induced by cadmium in skin epidermal cells.

There is accumulated evidence showing that cadmium leads to the generation of ROS, such as hydroxyl radicals (·OH), $O_2^{\cdot-}$, nitric oxide (NO), and H_2O_2 (Galan *et al*., 2001; O'Brien and Salacinski, 1998; Stohs *et al*., 2001). The mechanism of ROS generation by cadmium in JB6 cells is unclear. One possible mechanism is through NADPH oxidase, which can generate H_2O_2 in cadmium-exposed JB6 cells. Our present study reveals that H_2O_2 was significantly generated in cadmium-exposed cells not significant for $O_2^{\cdot-}$ and that CAT strongly inhibited cadmium-induced cytotoxicity. These results indicate that H_2O_2 generated by cadmium is closely involved in cadmium-induced apoptosis. With regards to this issue, it should be noted that AIF plays a critical role in ROS-stimulated cell death. We previously reported that continuously generated H_2O_2 induces caspase-independent AIF-mediated cell death in human lymphoma cells (Son *et al*., 2009). Moreover, the low and continuous generation of H_2O_2 converts the mode of cell death from caspase-dependent to caspase-independent cell death in cells exposed to a bolus of H_2O_2 (Barbouti *et al*., 2007). Due to this, we suggest that cadmium might generate H_2O_2 in low and continuous manner and AIF participates in the cadmium-induced apoptosis instead of executive caspase activation.

An interesting result of this study is that the upregulation of growth arrest and DNA damage–inducible protein 45α (GADD45α) expression is closely involved in the cadmium-induced apoptosis of skin epidermal cells. GADD45 has three isoforms, including GADD45α, -β, and -γ. These proteins were originally described as p53-dependent and stress-inducible genes (Smith *et al*., 1994). A variety of other transcription factors also regulate the expression of GADD45 (Thyss *et al*., 2005; Zerbini *et al*., 2004). Considerable evidence has documented that GADD45α has important roles in the induction of apoptosis (Hildesheim *et al*., 2002), where its transcription and functions are controlled either by JNK1 or JNK2 (Zhang *et al*., 2006). Our current study shows that cadmium dramatically increased the expression of GADD45α in skin epidermal cells, which is suppressed by blocking JNK with its pharmacological inhibitor or si-JNK transfection. The inhibition of GADD45α expression is more dramatic when these cells were transfected with si-JNK2 rather than with si-JNK1, whereas CAT did not affect its expression. Furthermore, the knockout of JNK2 rather than of JNK1 leads to a strong inhibition against cadmium-induced cytotoxicity. This suggests that the JNK-mediated pathway is critical for the upregulation of GADD45α and for the subsequent induction of apoptosis in cadmium-exposed cells, while this process is not affected by H_2O_2 generated by the metal. In addition, the JNK- and GADD45α-mediated signaling cascade does not appear to be related to the p53-mediated pathway. This is because a p53 inhibition by pharmacological inhibitor, PFT-α, or si-p53 transfection did not reduce the cadmium-mediated GADD45α upregulation, in spite of the significant increase in cell viability by inhibiting p53 in cadmium-exposed cells.

On the other hand, intracellular calcium homeostasis is very important in maintaining normally the cellular functions in response to extragenous and/or endogenous stimuli. It has been reported that cadmium increases intracellular levels of calcium ion, which mediates apoptosis in various types of cells (Kim and Sharma, 2004; Lemarie *et al*., 2004; Li *et al*., 2000; Shih *et al*., 2005; Wang *et al*., 2008). The present study supports the critical role of calcium ions in cadmium-induced apoptosis in

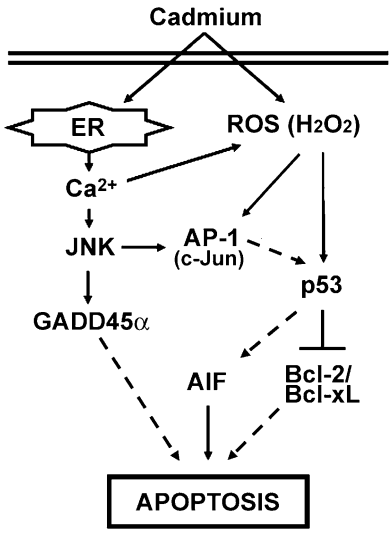

FIG. 9. Signal transduction pathways involved in cadmium-induced apoptosis in skin epidermal cells. Cadmium generates both calcium ions and H_2O_2. The calcium ions regulate JNK signaling and also effect H_2O_2 generation. H_2O_2 generated by cadmium regulates both AP-1 and p53 pathways in JB6 cells. Collectively, cadmium induces apoptosis mainly through calcium-JNK-GADD45α and a H_2O_2-AP-1-p53-Bcl-2/Bcl-xL signaling cascades. In addition, JNK-AP-1-p53 and ROS-p53-AIF signaling pathways play important roles in cadmium-induced apoptosis of the cells.

skin epidermal cells. Since cadmium elevates intracellular calcium levels and Bapta-AM protects cells from cadmium-induced cytotoxicity, the increase of free calcium ions is believed to be one of the main mechanisms involved in cadmium-induced apoptosis. It is likely that such increases in free calcium ions also causes apoptosis in cadmium-treated cells by stimulating the generation of H_2O_2. This is confirmed by the observations that levels of H_2O_2 generated were reduced by adding Bapta-AM into the cultures, whereas CAT did not decrease the intracellular calcium level in cadmium-exposed skin epidermal cells. Therefore, cadmium stimulates the increase of intracellular calcium ions in a ROS-independent manner. Calcium ions also lead to the activation of mitogen-activated protein kinases (MAPKs) in cadmium-exposed mesangial cells (Wang *et al.*, 2008) and in tributylin-treated human T-cell lines (Yu *et al.*, 2000). Similarly, our study shows that JNK activation was increased by calcium ions in cadmium-exposed cells. The prevention of JNK expression with pharmacological inhibitors or transfection with JNK-specific si-RNA attenuates cadmium-induced cytotoxicity and apoptosis in skin epidermal cells. A novelty of this study is that increased calcium ions by cadmium significantly regulated JNKs among MAPKs, and we further confirmed the important of JNK using si-RNA transfection in skin epidermal cells.

Our present data reveal that both JNK- and p53-mediated pathways are critical for the induction of apoptosis in cadmium-exposed cells, where calcium ions and H_2O_2 act as the pivotal mediators. Thus, we determined the downstream signaling pathways stimulated by JNK in cadmium-exposed cells. Our findings suggest that in addition to the upregulation of GADD45α expression, JNK stimulates the phosphorylation of c-Jun and the subsequent activation of AP-1, which is not affected by p53 activation. Taken together, this study suggests that several signaling cascades are affected by cadmium in skin epidermal cells.

In summary, this study shows that cadmium induces apoptosis through the caspase-independent mitochondria-mediated pathway in skin epidermal cells, where the decrease of Bcl-2/Bcl-xL, the upregulation of GADD45α, and the nuclear translocation of AIF are the critical events for apoptosis induction (Fig. 9). To our knowledge, this is the first report to demonstrate that p53- and JNK-mediated signaling acts as the pivotal apoptotic cell death, and this signaling is tightly affected by H_2O_2- and calcium-free ions generated by cadmium in skin epidermal cells. Therefore, our research indicates that p53 and JNK may be key therapeutic target molecules protecting skin against heavy metal–exposed skin disorders, such as skin ulcer, redness, and swelling.

FUNDING

National Institutes of Health (R01ES015518, 1R01CA119028, and 1R01CA116697).

ACKNOWLEDGMENTS

We thank Dr. Min Ding for stably transfected JB6 cells with AP-1-luciferase reporter plasmid.

REFERENCES

Bagchi, D., Joshi, S. S., Bagchi, M., Balmoori, J., Benner, E. J., Kuszynski, C. A., and Stohs, S. J. (2000). Cadmium- and chromium-induced oxidative stress, DNA damage, and apoptotic cell death in cultured human chronic myelogenous leukemic K562 cells, promyelocytic leukemic HL-60 cells, and normal human peripheral blood mononuclear cells. *J. Biochem. Mol. Toxicol.* **14,** 33–41.

Barbouti, A., Amorgianiotis, C., Kolettas, E., Kanavaros, P., and Galaris, D. (2007). Hydrogen peroxide inhibits caspase-dependent apoptosis by inactivating procaspase-9 in an iron-dependent manner. *Free Radic. Biol. Med.* **43,** 1377–1387.

Berridge, M. J., Bootman, M. D., and Lipp, P. (1998). Calcium—a life and death signal. *Nature* **395,** 45–648.

Ding, M., Shi, X., Dong, Z., Chen, F., Lu, Y., Castranova, V., and Vallyathan, V. (1999). Freshly fractured crystalline silica induces activator protein-1 activation through ERKs and p38 MAPK. *J. Biol. Chem.* **274,** 30611–30616.

Ercal, N., Gurer-Orhan, H., and Aykin-Burns, N. (2001). Toxic metals and oxidative stress part I: mechanisms involved in metal-induced oxidative damage. *Curr. Top. Med. Chem.* **1,** 529–539.

Fujimaki, H., Ishido, M., and Nohara, K. (2000). Induction of apoptosis in mouse thymocytes by cadmium. *Toxicol. Lett.* **115,** 99–105.

Galan, A., Garcia-Bermejo, L., Troyano, A., Vilaboa, N. E., Fernandez, C., de Blas, E., and Aller, P. (2001). The role of intracellular oxidation in death induction (apoptosis and necrosis) in human promonocytic cells treated with stress inducers (cadmium, heat, X-rays). *Eur. J. Cell Biol.* **80,** 312–320.

Galluzzi, L., Morselli, E., Kepp, O., Tajeddine, N., and Kroemer, G. (2008). Targeting p53 to mitochondria for cancer therapy. *Cell Cycle* **7,** 1949–1955.

Gerhardsson, L., Englyst, V., Lundstrom, N. G., Sandberg, S., and Nordberg, G. (2002). Cadmium, copper and zinc in tissues of deceased copper smelter workers. *J. Trace Elem. Med. Biol.* **16,** 261–266.

Gong, Q., and Hart, B. A. (1997). Effect of thiols on cadmium-induced expression of metallothionein and other oxidant stress genes in rat lung epithelial cells. *Toxicology* **119,** 179–191.

Hewison, M., Dabrowski, M., Vadher, S., Faulkner, L., Cockerill, F. J., Brickell, P. M., O'Riordan, J. L., and Katz, D. R. (1996). Antisense inhibition of vitamin D receptor expression induces apoptosis in monoblastoid U937 cells. *J. Immunol.* **156,** 4391–4400.

Hildesheim, J., Bulavin, D. V., Anver, M. R., Alvord, W. G., Hollander, M. C., Vardanian, L., and Fornace, A. J., Jr. (2002). Gadd45a protects against UV irradiation-induced skin tumors, and promotes apoptosis and stress signaling via MAPK and p53. *Cancer Res.* **62,** 7305–7315.

Hossain, S., Liu, H. N., Nguyen, M., Shore, G., and Almazan, G. (2009). Cadmium exposure induces mitochondria-dependent apoptosis in oligodendrocytes. *Neurotoxicology* **30,** 544–554.

Jarup, L. (2003). Hazards of heavy metal contamination. *Br. Med. Bull.* **68,** 167–182.

Kim, J., and Sharma, R. P. (2004). Calcium-mediated activation of c-Jun NH2-terminal kinase (JNK) and apoptosis in response to cadmium in murine macrophages. *Toxicol. Sci.* **81,** 518–527.

Lee, W. K., Abouhamed, M., and Thevenod, F. (2006). Caspase-dependent and -independent pathways for cadmium-induced apoptosis in cultured kidney proximal tubule cells. *Am. J. Physiol. Renal Physiol.* **291,** F823–F832.

Lemarie, A., Lagadic-Gossmann, D., Morzadec, C., Allain, N., Fardel, O., and Vernhet, L. (2004). Cadmium induces caspase-independent apoptosis in liver Hep3B cells: role for calcium in signaling oxidative stress-related impairment of mitochondria and relocation of endonuclease G and apoptosis-inducing factor. *Free Radic. Biol. Med.* **36,** 1517–1531.

Li, J. J., Westergaard, C., Ghosh, P., and Colburn, N. H. (1997). Inhibitors of both nuclear factor-kappaB and activator protein-1 activation block the neoplastic transformation response. *Cancer Res.* **57,** 3569–3576.

Li, M., Kondo, T., Zhao, Q. L., Li, F. J., Tanabe, K., Arai, Y., Zhou, Z. C., and Kasuya, M. (2000). Apoptosis induced by cadmium in human lymphoma U937 cells through Ca2+-calpain and caspase-mitochondria-dependent pathways. *J. Biol. Chem.* **275,** 39702–39709.

Mao, W. P., Ye, J. L., Guan, Z. B., Zhao, J. M., Zhang, C., Zhang, N. N., Jiang, P., and Tian, T. (2007). Cadmium induces apoptosis in human embryonic kidney (HEK) 293 cells by caspase-dependent and -independent pathways acting on mitochondria. *Toxicol. In Vitro* **21,** 343–354.

O'Brien, P., and Salacinski, H. J. (1998). Evidence that the reactions of cadmium in the presence of metallothionein can produce hydroxyl radicals. *Arch. Toxicol.* **72,** 690–700.

Polyak, K., Xia, Y., Zweier, J. L., Kinzler, K. W., and Vogelstein, B. (1997). A model for p53-induced apoptosis. *Nature* **389,** 300–305.

Qian, Y., Luo, J., Leonard, S. S., Harris, G. K., Millecchia, L., Flynn, D. C., and Shi, X. (2003). Hydrogen peroxide formation and actin filament reorganization by Cdc42 are essential for ethanol-induced in vitro angiogenesis. *J. Biol. Chem.* **278,** 16189–16197.

Shaikh, Z. A., Vu, T. T., and Zaman, K. (1999). Oxidative stress as a mechanism of chronic cadmium-induced hepatotoxicity and renal toxicity and protection by antioxidants. *Toxicol. Appl. Pharmacol.* **154,** 256–263.

Shih, C. M., Wu, J. S., Ko, W. C., Wang, L. F., Wei, Y. H., Liang, H. F., Chen, Y. C., and Chen, C. T. (2003). Mitochondria-mediated caspase-independent apoptosis induced by cadmium in normal human lung cells. *J. Cell. Biochem.* **89,** 335–347.

Shih, Y. L., Lin, C. J., Hsu, S. W., Wang, S. H., Chen, W. L., Lee, M. T., Wei, Y. H., and Shih, C. M. (2005). Cadmium toxicity toward caspase-independent apoptosis through the mitochondria-calcium pathway in mtDNA-depleted cells. *Ann. N. Y. Acad. Sci.* **1042,** 497–505.

Smith, M. L., Chen, I. T., Zhan, Q., Bae, I., Chen, C. Y., Gilmer, T. M., Kastan, M. B., O'Connor, P. M., and Fornace, A. J., Jr. (1994). Interaction of the p53-regulated protein Gadd45 with proliferating cell nuclear antigen. *Science* **266,** 1376–1380.

Son, Y. O., Jang, Y. S., Heo, J. S., Chung, W. T., Choi, K. C., and Lee, J. C. (2009). Apoptosis-inducing factor plays a critical role in caspase-independent, pyknotic cell death in hydrogen peroxide-exposed cells. *Apoptosis* **14,** 796–808.

Stohs, S. J., and Bagchi, D. (1995). Oxidative mechanisms in the toxicity of metal ions. *Free Radic. Biol. Med.* **18,** 321–336.

Stohs, S. J., Bagchi, D., Hassoun, E., and Bagchi, M. (2001). Oxidative mechanisms in the toxicity of chromium and cadmium ions. *J. Environ. Pathol. Toxicol. Oncol.* **20,** 77–88.

Susin, S. A., Lorenzo, H. K., Zamzami, N., Marzo, I., Snow, B. E., Brothers, G. M., Mangion, J., Jacotot, E., Costantini, P., Loeffler, M., *et al.* (1999). Molecular characterization of mitochondrial apoptosis-inducing factor. *Nature* **397,** 441–446.

Szuster-Ciesielska, A., Stachura, A., Slotwinska, M., Kaminska, T., Sniezko, R., Paduch, R., Abramczyk, D., Filar, J., and Kandefer-Szerszen, M. (2000). The inhibitory effect of zinc on cadmium-induced cell apoptosis and reactive oxygen species (ROS) production in cell cultures. *Toxicology* **145,** 159–171.

Thyss, R., Virolle, V., Imbert, V., Peyron, J. F., Aberdam, D., and Virolle, T. (2005). NF-kappaB/Egr-1/Gadd45 are sequentially activated upon UVB irradiation to mediate epidermal cell death. *EMBO J.* **24,** 128–137.

Wang, S. H., Shih, Y. L., Ko, W. C., Wei, Y. H., and Shih, C. M. (2008). Cadmium-induced autophagy and apoptosis are mediated by a calcium signaling pathway. *Cell. Mol. Life Sci.* **65,** 3640–3652.

Wang, S. H., Shih, Y. L., Lee, C. C., Chen, W. L., Lin, C. J., Lin, Y. S., Wu, K. H., and Shih, C. M. (2009). The role of endoplasmic reticulum in cadmium-induced mesangial cell apoptosis. *Chem. Biol. Interact.* **181,** 45–51.

Wang, Y., Fang, J., Leonard, S. S., and Rao, K. M. (2004). Cadmium inhibits the electron transfer chain and induces reactive oxygen species. *Free Radic. Biol. Med.* **36,** 1434–1443.

Watjen, W., Haase, H., Biagioli, M., and Beyersmann, D. (2002). Induction of apoptosis in mammalian cells by cadmium and zinc. *Environ. Health Perspect.* **110,** 865–867.

Xu, C., Johnson, J. E., Singh, P. K., Jones, M. M., Yan, H., and Carter, C. E. (1996). In vivo studies of cadmium-induced apoptosis in testicular tissue of the rat and its modulation by a chelating agent. *Toxicology* **107,** 1–8.

Yakovlev, A. G., Wang, G., Stoica, B. A., Boulares, H. A., Spoonde, A. Y., Yoshihara, K., and Smulson, M. E. (2000). A role of the Ca2+/Mg2+-dependent endonuclease in apoptosis and its inhibition by poly(ADP-ribose) polymerase. *J. Biol. Chem.* **275,** 21302–21308.

Yin, X. M., Wang, K., Gross, A., Zhao, Y., Zinkel, S., Klocke, B., Roth, K. A., and Korsmeyer, S. J. (1999). Bid-deficient mice are resistant to Fas-induced hepatocellular apoptosis. *Nature* **400,** 886–891.

Yu, Z. P., Matsuoka, M., Wispriyono, B., Iryo, Y., and Igisu, H. (2000). Activation of mitogen-activated protein kinases by tributyltin in CCRF-CEM cells: role of intracellular Ca(2+). *Toxicol. Appl. Pharmacol.* **168,** 200–207.

Zamzami, N., Marchetti, P., Castedo, M., Decaudin, D., Macho, A., Hirsch, T., Susin, S. A., Petit, P. X., Mignotte, B., and Kroemer, G. (1995). Sequential reduction of mitochondrial transmembrane potential and generation of reactive oxygen species in early programmed cell death. *J. Exp. Med.* **182,** 367–377.

Zerbini, L. F., Wang, Y., Czibere, A., Correa, R. G., Cho, J. Y., Ijiri, K., Wei, W., Joseph, M., Gu, X., Grall, F., *et al.* (2004). NF-kappa B-mediated repression of growth arrest- and DNA-damage-inducible proteins 45alpha and gamma is essential for cancer cell survival. *Proc. Natl. Acad. Sci. U.S.A.* **101,** 13618–13623.

Zhang, D., Song, L., Li, J., Wu, K., and Huang, C. (2006). Coordination of JNK1 and JNK2 is critical for GADD45alpha induction and its mediated cell apoptosis in arsenite responses. *J. Biol. Chem.* **281,** 34113–34123.